INSTITUTE OF PLASMA PHYSICS

NAGOYA UNIVERSITY

# RESEARCH REPORT

NAGOYA, JAPAN

# ELECTRON DENSITY MEASUREMENT OF A TOKAMAK PLASMA BY AN HCN LASER INTERFEROMETER

Akimitsu NISHIZAWA, Masaru MASUZAKI
and
Akihiro MOHRI

IPPJ-244 April 1976

Further communication about this report is to be sent to the Research Information Center, Institute of Plasma Physics, Nagoya University, Nagoya, Japan.

# Error — Correction Table

| Page | column | error | correction |
|---|---|---|---|
| 1 | 8 | $cm^3$ | $cm^{-3}$ |
| | 24 | $cm^3$ | $cm^{-3}$ |
| 9 | 15 | $cm^3$ | $cm^{-3}$ |
| 10 | 19 | mudulated | modulated |
| 11 | 5 | $(1-e^{-t})$ 100% | $(1-e^{-t})\times 100\%$ |
| | 8 | $cm^3$ | $cm^{-3}$ |
| | 11 | 1.2 $m$ | 1.2 $\mu$m |
| | 21 | follows: | follows. |
| 13 | 20 | spide | spike |
| 14 | 10 | one turn—loop | one—turn—loop |
| 15 | 19 | was 2 | was |
| | 21 | $cm^3$ | $cm^{-3}$ |
| 17 | 24 | D. Veron: | D. Veron, |

Abstract:

An HCN-laser interferometer has been constructed for the electron density measurement of plasmas. The output power of the HCN laser has been stabilized to be fit for long-term operation. The interferometer is of Michelson-type with a concave mirror as the reflecting mirror so as to reduce the refractive effect due to plasmas. The mean electron density of SPAC-II tokamak plasma ($3 \sim 7.5 \times 10^{13}$ cm$^3$) was measured by this interferometer. The signal-to-noise ratio was 20, which was mainly determined by the fluctuation of the laser output power. Changes of the phase shift corresponding voltage spikes in the one-turn-loop voltage signal were also observed.

## §1. INTRODUCTION

Until now, microwave interferometers have been convenient tools for the electron density measurement of tokamak plasmas. However, as a result of recent tokamak researches, both the electron density and the plasma diameter have so increased that it becomes an urgent problem to develop interferometers which use far infrared light, such as the HCN-laser beam of wave length of 337 μm, as a probing beam. An infrared-laser interferometer has the following advantages as compared with a microwave interferometer: its cut-off density is higher, the phase shift due to plasma is linear for the density lower than $10^{15}$ cm$^3$ and the refractive effect caused by the density gradient is smaller.[1] Moreover, owing to the coherency, divergence of the probe beam is smaller and the beam can be waisted much thinner, so that better spatial resolution can be obtained.

This paper gives a description on the construction of an HCN-laser interferometer of Michelson-type and its application to the electron density measurement of a tokamak called SPAC-II.

The Michelson-type interferometer has such an advantage over the Mach-Zehnder type one[1] that its sensitivity to the phase shift is better than that of the latter because of the double travel of the beam through plasma, although the decrease of the beam intensity due to the attenuation and the reflection by windows and lenses is larger for the former than for the latter. Furthermore, as stated in the section 2.3, in the former the refractive effect of the beam due to the electron density gradient is reduced by using a concave mirror as reflecting mirror in the plasma path.

The following section gives a description on the HCN laser, including the alignment of its optical components and optical properties of the interferometer. In §3, experimental results are given for its application to the SPAC-II plasma.

## §2. THE HCN LASER INTERFEROMETER

In this section, the laser system used in the experiment is described. In order to obtain reliable results for a long experimental period and during each measurement time of order of 10 msec, stabilization of the laser power[2,3,4] is necessary. Some improvements on these points are made.

### 2.1.1 Outline of the HCN Laser

A schematic diagram of the HCN laser apparatus used is shown in Fig. 1. The resonator of the HCN laser is a Fabry-Perot interferometer with a pair of parallel plane mirrors[5] which

are coated with aluminium. The effective radius of each mirror is 50 mm and the cavity length is 240 cm. One of the mirror set in the vacuum tank, which is called the tuning mirror, is movable along the laser axis for tuning the resonator. Its angle to the laser axis can be adjusted by rotating it vertically (tilting) and horizontally, tilting being adjustable from the outside through a vacuum seal. The tilt angle of the mirror to the laser axis is kept within 5 seconds when it is shifted along the axis. The other mirror, which is called tilting mirror, is jointed on the end of the Pyrex discharge tube opposite to the vacuum tank with a bellows. The angle of this mirror to the axis of the laser is adjustable with three adjusting screws which are mounted on the mirror support. This system has an advantage that the surplus transverse forces which would result from the rotation of adjusting screws, if they were attached directly to the tilting mirror holder, are eliminated and the mirror is accurately moved. At the center of this mirror, there is a transparent circular area 2 mm in diameter for aligning the optical system with a He-Ne laser. This area has little influence on the laser power.

A gas mixture composed of $N_2$, $CH_4$ and He is introduced into the discharge tube from the inlet at the anode side. The mixing ratio of $N_2$ and $CH_4$ is 3:2 and the partial pressure of helium gas is a few times higher than that of the lasing gas. Typical discharge conditions are as follows: the flowing rate of the gas mixture is 20 atm$\cdot$cm$^3$/min with the fluctuation kept less than a few percent; the gas pressure is 0.8 torr at the outlet of the discharge tube; and the discharge current and the

discharge voltage are 0.6 A and 800 V respectively. In order to monitor the discharge condition in connection with the pressure variation, observation of the "fish bone", which appears when the discharge changes from the positive column phase to the arc phase, is found to be useful. When the discharge current is fixed at 0.6 A, the whole discharge tube is filled with positive column at a pressure of 0.75 torr. As the gas pressure increases with the flow rate, the "fish bone" appears first in front of the anode and gradually extends toward the cathode. At a pressure of 0.9 torr, the "fish bone" reaches the cathode. The length of the "fish bone" increases at a rate of about 10 cm per 0.01 torr, but this rate is not exactly constant and is a little sensitive to the discharge power. It should be noticed that the "fish bone" length is little affected even when much helium gas is mixed with the lasing gas, probably because the length of the "fish bone" depends mainly on the pressure gradient of $CH_4$ and $N_2$ gases because of the small mass of a helium atom.

The laser beam is extracted out by a coupling mirror of 15 mm in diameter which is placed in the laser cavity. The laser output power becomes maximum when the ratio of the coupling mirror area to the cavity mirror area is 0.1,[6] and was a few mW.

2.1.2 Stabilization of the Laser Power

In order to stabilize the output power of the HCN laser for a long term of measurement, the following contrivances are done.

a) Thermal stabilization —— In order to avoid the disturbance of the magnetic field for plasma confinement due to the laser apparatus, the laser bench 2.5 m in length is made of aluminium (the thermal expansion is 50 $\mu m/^{o}C$). Because the tuning width of the laser in the CW operation is 8 $\mu m$, the change of the length between cavity mirrors with a temperature fluctuation is the most serious problem. In order to reduce the temperature effect on the cavity length, the spacers between the two cavity mirrors are made of four fused quartz cylinders[4,7] 2 m in length and 4 cm in diameter. One of the mirror supports (the vacuum tank) is fixed on the bench, and the other is freed to slide along the bench. The thermal expansion of the discharge tube is absorbed by the bellows. As the result, the change of the cavity length becomes less than 1 $\mu m/^{o}C$, which means that the relative change of the laser power is reduced to 1/100 or less for the temperature variation of several-tenths of one degree, C. In addition, the discharge tube is water-cooled to decrease the heating of the quartz supports by the thermal radiation from the discharge.

b) Mechanical stabilization —— By using the four quartz cylinders as the spacers between the two cavity mirrors, the movement of the mirrors which may be caused by bending and oscillation of the bench can be held parallel and also the oscillation of the cavity length is kept small.

c) Stabilization of discharge condition —— Helium gas is mixed with the lasing gas.[7,8]* The partial pressure of

---

* It is reported that by mixing helium gas the laser power can be increased.[3] But in our case, the laser output scarcely increases under the condition that the discharge power is constant, as in the case of Ref. 7.

helium is a few times higher than that of the lasing gas. Since the mass of a helium atom or ion is lighter than that of CN radical, helium may have an effect of stabilizing the space potential distribution of the laser plasma. Helium gas also works to clean the wall of the discharge tube.[7] In order to obtain the stabilized discharge, sputtering on the cathode surface should be reduced, too. For this purpose, a modified hollow cathode as shown in Fig. 1 is used. Sputtering on the cathode surface is reduced owing to the increase of the surface area and the presence of the jutting part. Vermicular damages of the "O" rings between each electrode and the discharge tube are suppressed by inserting water-cooled flanges between each electrode and the discharge tube.

In consequence of these efforts, the change of the laser power has become less than a few percent for at least ten hours. The power fluctuation mostly found in the frequency range of kilo-Hertz has been about 0.5 %.

## 2.2 Alignment of the Optical Components and Optical Properties of the HCN Laser

The alignment of the optical components is one of the most important problems for the measurement. Large laser output is realized by optimizing the alignment of the cavity mirrors. At the same time, the laser beam must pass through the center of the viewing windows of the plasma device which are located far from the laser and the visibility of interference must be maximized at the interferometer.

The alignment was performed by the following processes. A He-Ne laser light was first passed through the transparent circular area at the center of the tilting mirror. Accuracy of parallelism of the pair of cavity mirrors was adjusted within 3 seconds by observing a He-Ne laser fringe on the tuning mirror. The tilting angle of the tilting mirror to the He-Ne laser beam was set less than 0.8 minutes by observing multireflected beam spots on the tilting mirror surface. The He-Ne laser beam was reflected out by the coupling mirror at a reflection angle of about $45^{\circ}$ with respect to the axis, and then was passed into the interferometer through a Myler sheet window. The coupling method with the coupling mirror is more convenient for the alignment of the interferometer than that with a coupling hole, because the direction of the reflected laser beam can be changed by rotating the coupling mirror.

In order to make the HCN laser axis coincide with the He-Ne laser beam at the interferometer, a near-field-pattern of the HCN laser beam[5] at a point of 100 cm from the coupling mirror was observed by scanning a Golay cell with an aperture of 2 mm in diameter in a plane perpendicular to the axis. The position of the maximum intensity was sometimes not on the path of the He-Ne laser beam and the deviation angle was larger than the tilting angle of the cavity mirrors to the He-Ne laser beam. According to the cavity theory by Fox et al.,[9] the tilt of the cavity mirrors makes the mode pattern asymmetric in the cavity and the diffraction loss becomes greater. Therefore it seems probable that due to the residual tilt angle of the mirrors to the He-Ne laser beam the path of the HCN laser beam

did not coincide with that of the He-Ne laser beam. In such a case, a Golay cell was placed to the position at which the He-Ne laser beam hit its window, and then the tilt of the cavity mirrors were finely adjusted so that the detected power was maximized, the parallelism being kept within 3 seconds. After the adjustment the maximum intensity became larger and the intensity distribution became more symmetric. The remaining asymmetry seemed to be due to the asymmetry of the radial density distribution of the laser plasma which was indicated by the asymmetry of the stationary plasma striation.

Divergence of the extracted laser beam from the coupling mirror was estimated from a far-field-pattern.[10] Figure 2 shows a far-field-pattern which was measured by scanning a Goley cell in a plane perpendicular to the beam which contains the focus of a lens, with a focal length of 170 mm, used to focus the laser beam. In Fig. 2 $TEM_{00}$ and $TEM_{10}$ mode are shown. The half-intensity width was estimated from

$$\frac{1}{2} d = f \tan \theta_{\frac{1}{2}} \tag{1}$$

where d, f and $\theta_{\frac{1}{2}}$ are the half-intensity width, the focal length and the divergence angle, respectively.

In Fig. 2, the divergence angle is 26 minutes. The theoretical value for the divergence angle is 2 degrees and 4 minutes for a coupling mirror with an effective diameter of 12 mm. This large difference between the experimental value and the theoretical one may be due to the difference between the actual intensity distribution in the laser cavity and the intensity distribution assumed in the theory.

## 2.3 Interferometer

The laser beam extracted with the coupling mirror is led to a Michelson-type interferometer (in Fig. 3), and is divided into two beams with a beam splitter made of Mylar sheet. One beam is led to the reference mirror. The other beam is focused at the center of the plasma by the telescope method with two polyethylene lenses with focal lengths of 35 cm and 100 cm respectively which are fixed on an aluminium bench 2 m long, reflected by a concave mirror with a radius of 35 cm, and refocused at the center of the plasma. The path length of the probing beam is 3.5 m in one way. The waisted spot of the laser beam at the center of the plasma is estimated to be 15 mm in diameter. The maximum refracted angle of the laser beam due to the lens effect of plasma[11] is $6 \times 10^{-4}$ radian for a parabolic density distribution with a density of $5 \times 10^{13}$ $cm^3$ at the center. But, as the refracted laser beam passes near the center of the plasma, the laser beam reflected by the concave mirror comes back near the same path. That is to say the Mychelson-type interferometer with a concave mirror has the advantage in the reduction of the lens effect due to the density gradient.

The two windows for observation are 30 mm in diameter and placed at a distance of 66 cm between them. The window material is Mylar sheet 100 μm thick for the He-Ne laser to be passable. The transparency of this Mylar sheet for the HCN laser is 70 %. The Mylar sheet is strong enough against the pressure difference and can be used at pressure lower than $10^{-7}$ torr because of little outgassing, although this sheet can not

be used in a hot place.

The laser beam which interferes with the reference beam is focused into the light pipe with a polyethylene lens and detected with an InSb crystal cooled with liquid helium. For the purpose of the phase setting of the reference beam, the reference mirror is finely movable parallel to the laser axis. The deviation of parallelism due to the parallel shift of the reference mirror is less than 10 seconds.

The intensity of probing beam decreases into 5 % after the double travel through two polyethylene lenses and two Mylar sheet windows. Therefore the reference beam was used without attenuating its intensity in order to increase the intensity of the interfered beam (the fringe).

For a transient plasma, the path of the laser beam returned through the plasma deflects by the lens effect of the plasma from the path of the incident beam, the deflection angle depending on time, and the path length changes too. So an additional phase shift arises due to this change of the path length. Also the amplitude of the fringe signal is mudulated by the change of the visibility because the position of the probing beam on the detector changes relative to that of the reference beam. Estimation is made of the degree of modulation of the amplitude of the fringe signal and of the phase shift due to the change of the path length as follows. For the gaussian type intensity distribution of the laser beam, the maximum amplitude of the fringe signal $I_\theta$ for the deflection angle $\theta$ of the returned beam is given by

$$I_\theta = I_o \, e^{-(t/4)(\theta L/a)^2}$$

where $I_o$ is the maximum amplitude for $\theta = 0$, L is the path length of the probing beam and $(1 - e^{-t})$ 100 % of the total intensity is included in the cylinder with a radius a. If we put $\theta = 6 \times 10^4$ radian, which corresponds to the peak density of $5 \times 10^{13}$ $cm^3$, a = 1 cm and $1 - e^{-t} = 0.98$, then $\theta L$ = 2 mm for L = 3.5 m, so $I_\theta / I_o = 0.96$. Therefore the amplitude of the fringe signal is modulated by 4 %. The change of the path length is 1.2 m in this case, which corresponds to 1/300 of one fringe.

## §3. MEASUREMENT OF THE ELECTRON DENSITY OF SPAC-II PLASMA

### 3.1 SPAC-II

SPAC-II is a tokamak type machine[12] with a major radius of 28 cm. The liner with an inner radius of 0.7 cm is made of stainless steel bellows of 0.3 mm thick. The limiter has an inner radius of 5.5 cm, and the shell of 1.5 cm thick is made of aluminium and has an inner radius of 8 cm. The base pressure is $2 \times 10^{-7}$ torr. The typical values of parameters are as follows: The peak of the toroidal magnetic field $B_t$ is 10 kG, the vertical magnetic field $B_v$ several tens gauss, the peak of the Ohmic-current $I_p$ around 15 kA, the electron conduction temperature, assuming $Z_{eff} = 2$, around 60 eV and the filling pressure of hydrogen gas of several times $10^{-4}$ torr.

### 3.2 Experimental Results

A schematic diagram of the experimental apparatus is shown in Fig. 3. In the electron density measurement, the phase

shift without the plasma was set at zero by shifting the reference mirror, and then the interfered light intensity with presence of the plasma was detected. The output of the InSb crystal detector was amplified by 20 times by an I.C. operational amplifier and displayed on an oscilloscope. The output corresponding to a half of one fringe was 30 mV. This value indicated that the power of the fringe signal to the detector was 1/200 of the original power.

A typical fringe profile is shown in Fig. 4(a), and the corresponding electron density is shown in Fig. 4(b) under the assumption that the plasma diameter was 11 cm.

The noise in the fringe signal displayed on an oscilloscope were mainly determined by the fluctuation of the laser power because the noise of the detector and the amplifier was negligibly small. Signal-to-noise ratio is determined as follows. The intensity of the laser beam introduced to the detector is given by

$$I = a_o^2 \gamma (1 \pm \beta^2)(1 - r^2) r^2 (1 + 2\alpha^2 \cos\phi),$$

where $a_0^2$ is the original power of the laser, $\beta^2$ the ratio of fluctuation, $r^2$ the reflectivity of the beam splitter, $\alpha^2$ the transmissivity of the probing beam, $\gamma$ transmissivity of the light pipe and $\phi$ the phase shift of the probing beam. As the amplifier of the detected signal is an AC amplifier, the amplifier amplifies not only $2\alpha^2 \cos\phi$, but also the laser fluctuation $\beta^2$. For $\alpha^2 << 1$ and $\beta^2 << 1$, the signal-to-noise ratio S/N is given by

$$S/N = 2\alpha^2/\beta^2.$$

In our case, as $\alpha^2 = 0.05$ and $\beta^2 \sim 0.005$, S/N = 20. This feature can be seen in the fringe signal shown in Fig. 8.

The mean electron density became maximum before the current reached its maximum, and not a little plasma remained without being extinguished after the current decreased to a small value. The maximum electron density increased with the filling pressure as shown in Fig. 5.

The fluctuation of the plasma was able to be observed as shown in Figures 6, 7, and 8. Figure 6 shows the fluctuation in the fringe signal correlating with the negative spikes [13] in the one-turn-loop voltage signal. In this case, the phase shift, which is proportional to $n_e\ell$ ($\ell$ is the path length), decreased by 20 % when the first negative spike occurred. The oscillation near the negative spike is shown in Figs. 6(c) and 7. The oscillation corresponded to that in the magnetic probe signal (the Mirnov oscillation).[13] The amplitude of the oscillation of the fringe signal grew gradually until the negative spide occurred, and disappeared at the spike. It grew again gradually and this process repeated itself. The amplitude of the magnetic probe signal also grew before the spike, but at the spike , on the contrary, it became larger instead of disappearing and decreased gradually after a while. The frequency of the oscillation is $3.3 \sim 6.6 \times 10^4$ Hz. The fluctuation of the $n_e\ell$ during the oscillation is $0.6 \times 10^{13}$ $cm^{-2}$ which is 12 % of $n_e\ell$. Fig. 8 shows the change of the fringe corresponding to the positive spike in the one-turn-loop

voltage. Each dip in the fringe was several percent of the total density, and such a drastic change of the fringe as occurred in the case of the negative spike did not appear.

An effect of injection of the relativistic electron beam (REB)[14] into the plasma is shown in Fig. 9. The part of jump in the fringe signal at the time of the injection of REB in the picture was found to be due to insufficient shielding of the amplifier. The mean electron density increased by a few percent when REB was injected. After about 100 μsec, a negative spike appeared, the one-turn-loop voltage increased drastically, the mean electron density decreased drastically, and the current decreased remarkably.

## §4. CONCLUSION

A Michelson-type HCN-laser interferometer has been constructed for the measurement of plasma electron density. The following improvements are made to stabilize the laser power for long-term operation.

(1) The change of the cavity length due to the temperature change is reduced by using four fused quartz cylinders of 2 m in length and 4 cm in diameter as spacers. (2) The change of the parallelism of the cavity mirrors and the oscillation of the cavity length due to mechanical oscillations are also reduced by these spacers. (3) The discharge is stabilized by mixing helium gas with the lasing gas in order to stabilize the spatial potential distribution and by using a modified hollow cathode in order to reduce sputtering on the cathode surface. As a result of these improvements the change of the laser power becomes less than a few percent for ten hours.

For the purpose of the alignment, the intensity distribution of the laser beam was measured. The property of the laser light as the probing beam was affected by the tilting angle of the laser cavity mirrors. The beam divergence may be made small by extracting a selected mode in the cavity.

The signal-to-noise ratio of the fringe signal depended mainly on the transmissivity of the probing beam and the fluctuation of the laser power, and was 20. This ratio may be increased by increasing the laser power and attenuating the reference beam power.

As the interferometer the Michelson-type was adopted, because its sensitivity to the phase shift is better than that of the Mach-Zehnder-type, and the refractive effect of the laser beam due to the electron density gradient is reduced by using a concave mirror as the reflecting mirror in the plasma path.

The mean electron density of SPAC-II plasma was determined by this interferometer. The phase shift due to the plasma was about one to three fringes when the filling pressure was 2 $\sim$ 8 $\times$ $10^{-4}$ torr, which corresponded to the mean electron density of 3 $\sim$ 7.5 $\times$ $10^{13}$ $cm^3$ under the assumption that the plasma diameter was 11 cm. The change of the phase shift were observed corresponding to nagative or positive spikes in the one-turn-loop voltage signals. Effects of injection of a relativistic electron beam into the plasma was also detected.

The present results show that an HCN-laser interferometer is a convenient method for the electron density measurement for present and future tokamaks.

As the refractive effect due to plasmas is smaller for the infrared light than for the microwave, the infrared laser interferometer can be used to know the density profile of the tokamak plasmas. For this purpose it is an urgent problem to develop a multi-channel interferometer, for which an infrared laser with an output power as much as 10 times of the present lasers should be developed.*

Veron[15] reported a method for displaying the phase shift with zebra pattern.* However, in order to detect fast transient phenomena such as oscillations relating to the disruptive instability, a fast recording method of phase shift should be necessary.

ACKNOWLEDGMENTS

The authors wish to thank Dr. S. Kon and Dr. M. Yamanaka for his helpful discussion, and Dr. J. Yamamoto for his generous advice of the detector. We are also grateful to Professor K. Takayama, Professor K. Matsuura, Professor J. Fujita and Professor M. Otsuka for their constant supports and Mr. Ukegawa and Mr. Kato for helping with the experiments.

---

* Subsequent to the completion of this work, we learned of the work of D. Veron et. al. who applied a multi-channel HCN laser interferometer to the electron density measurement of TFR plasma.[16]

References


1) P. Brossier and R. A. Blanken: IEEE Transaction on Microwave Theory and Techniques MTT-22 (1974) 1053.

2) D. T. Lewellyn-Jones and M. D. James: J. Phys. E5 (1972) 468.

3) K. Yoshihiro and C. Yamanouchi: Rev. Sci. Instr. 45 (1974) 767.

4) J. P. Lesieur, M. C. Sexton and D. Veron: J. Phys. D5 (1972) 1212.

5) M. Yamanaka, H. Yoshinaga and S. Kon: Japan J. Appl. Phys 7 (1968) 250.

6) S. Kon, M. Yamanaka, J. Yamamoto and H. Yoshinaga: Japanese J. Appl. Phys. 6 (1967) 612.

7) P. Belland and D. Veron: Opt. Comm. 9 (1973) 146.

8) P. Belland, A. I. Ciura and L. B. Whitbourn: Opt. Comm. 11 (1974) 21.

9) A. G. Fox and T. Li: Proc. IEEE 51 (1963) 80.

10) D. R. Harrott: J. Opt. Soc. 52 (1962) 31.

11) J. Shmoys: J. Appl. Phys. 32 (1961) 689.

12) Y. Hamada and A. Mohri: Japanese J. Appl. Phys. 13 (1974) 1624.

13) See H. P. Furth: Nuclear Fusion 15 (1975) 487.

14) M. Masuzaki, A. Mohri, T. Tsuzuki, A. Nishizawa and K. Ikuta: Proc. of the 7th European Conference on Controlled Fusion and Plasma Physics, Lausanne, 1975, Vol. 1, p.17.

15) D. Veron: Opt. Comm. 10 (1974) 95.

16) D. Veron: J. Certain and J. P. Crenn: Laboratory Report EUR-CEA-FC-799 (1975).

## FIGURE CAPTIONS

Fig. 1. Schematic diagram of the HCN laser.

Fig. 2. Radial distribution of the HCN laser beam which is extracted with the coupling mirror.

Fig. 3. Schematic diagram of the experimental system.

Fig. 4. (a) A typical fringe signal F. (b) the mean electron density estimated from the fringe numbers.

Fig. 5. The pressure dependence of the maximum value of the mean electron density.

Fig. 6. (a) Behaviors of the fringe signal near the negative spike. The loop voltage $V_\ell$ (20 V/div), the discharge current $I_p$ (10 kA/div) and the horizontal shift $S_h$. The arrow shows the positive direction for the respective values except for $S_h$ (the inward direction for $S_h$). (b) the mean electron density and (c) the oscillation near the negative spike in the magnetic probe MP, and the fringe. Sweep time is 20 μsec/div. The filling pressure was $2 \times 10^{-4}$ torr.

Fig. 7. The oscillation near the negative spike in the magnetic probe signal, and the fringe.

Fig. 8. The change of the fringe at the positive spike (marked by ↑) and the mean electron density.

Fig. 9. The effect on the fringe of the injection of a relative electron beam (REB) (marked by ↑).

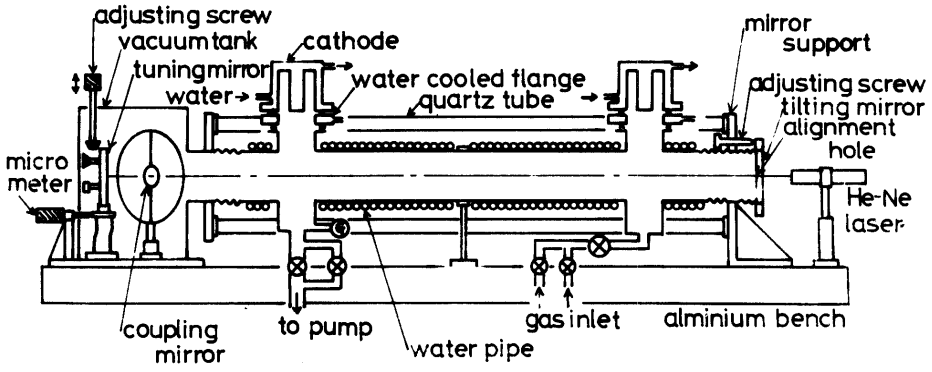
adjusting screw
vacuum tank
tuning mirror
water
cathode
water cooled flange
quartz tube
mirror support
adjusting screw
tilting mirror
alignment hole
micro meter
He-Ne laser
coupling mirror
to pump
water pipe
gas inlet
alminium bench

Fig. 1

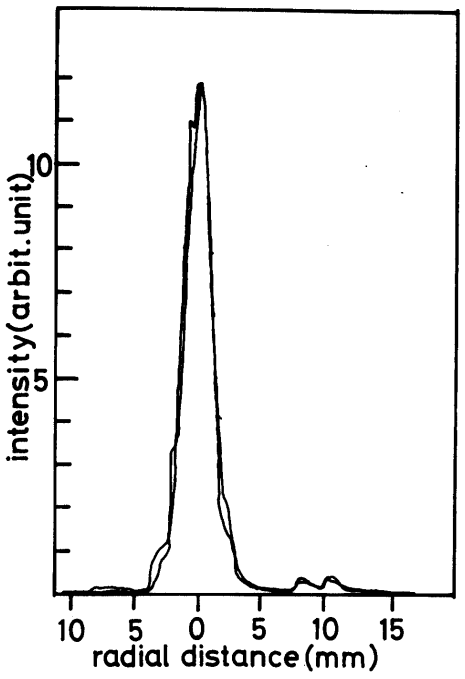


Fig. 2

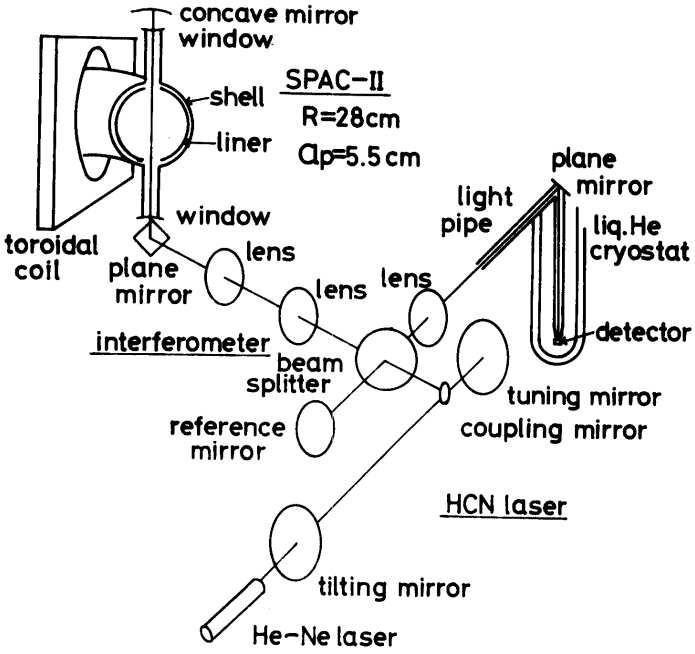
concave mirror
window
SPAC-II
shell
R=28cm
liner
ap=5.5 cm
plane
mirror
light
pipe
liq.He
cryostat
window
toroidal
coil
lens
plane
mirror
lens
lens
interferometer
detector
beam
splitter
tuning mirror
coupling mirror
reference
mirror
HCN laser
tilting mirror
He-Ne laser

Fig. 3

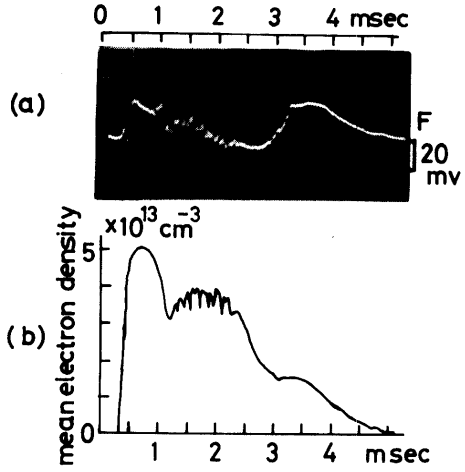
0 1 2 3 4 msec
(a)
F
20
mv
x10^13 cm^-3
5
(b)
mean electron density
0
1 2 3 4 msec

Fig. 4

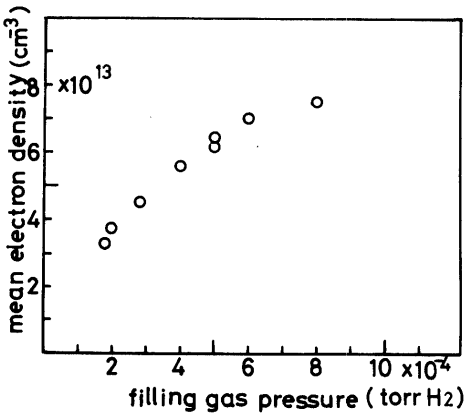
mean electron density (cm⁻³)
x10¹³
8
6
4
2
2
4
6
8
10 x10⁻⁴
filling gas pressure ( torr H2)

Fig. 5

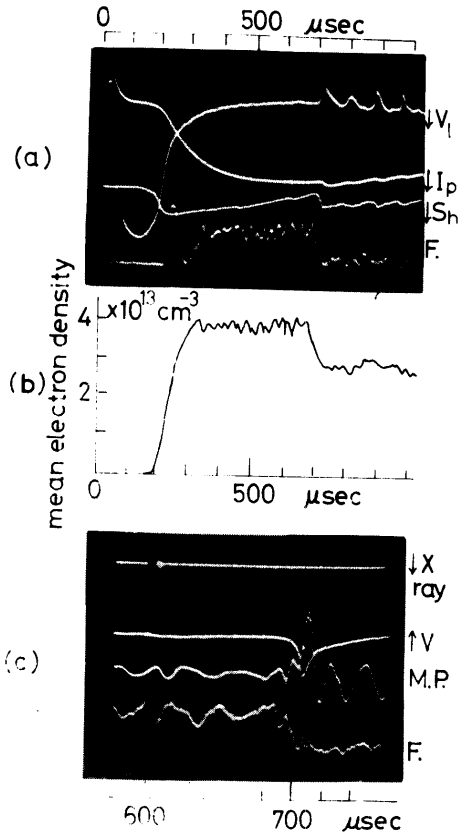
0
500 μsec
(a)
$V_l$
$I_p$
$S_h$
F.
mean electron density
$\times 10^{13}$ cm$^{-3}$
4
2
(b)
0
500 μsec
(c)
X ray
V
M.P.
F.
600
700 μsec

Fig. 6

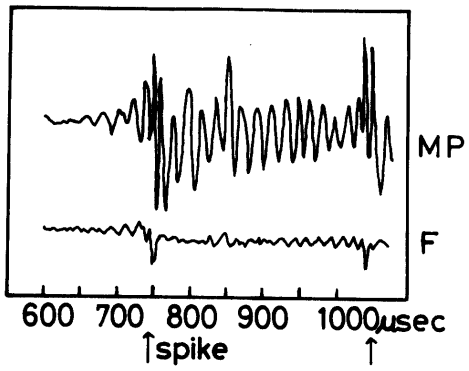


Fig. 7

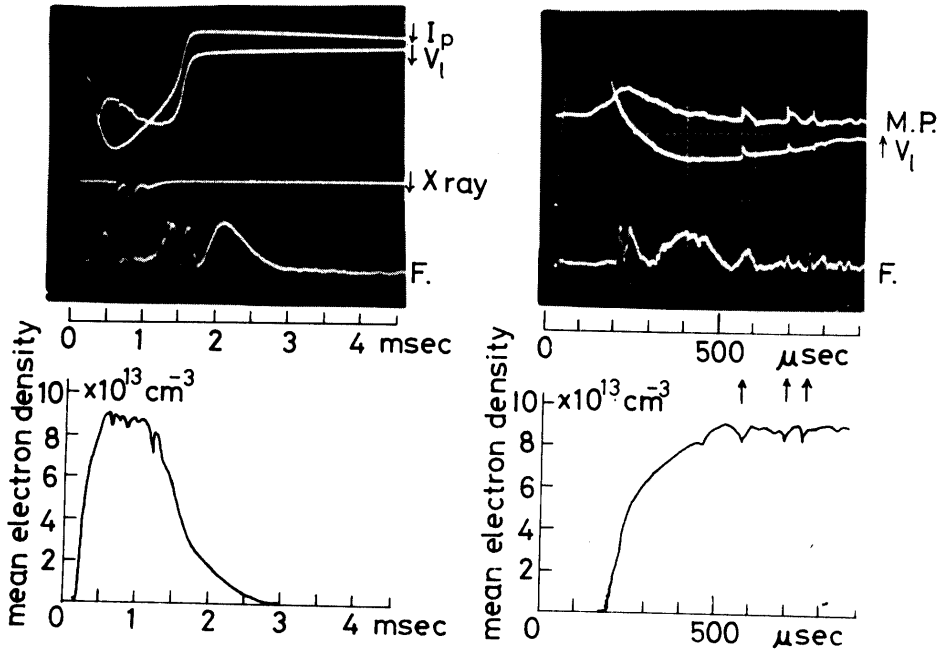
↓ $I_p$
↓ $V_l$
↓ X ray
F.
0 1 2 3 4 msec
mean electron density
x10$^{13}$cm$^{-3}$
10
8
6
4
2
0 1 2 3 4 msec
M.P.
↑ $V_l$
F.
0 500 μsec
mean electron density
x10$^{13}$cm$^{-3}$
10
8
6
4
2
0 500 μsec

Fig. 8

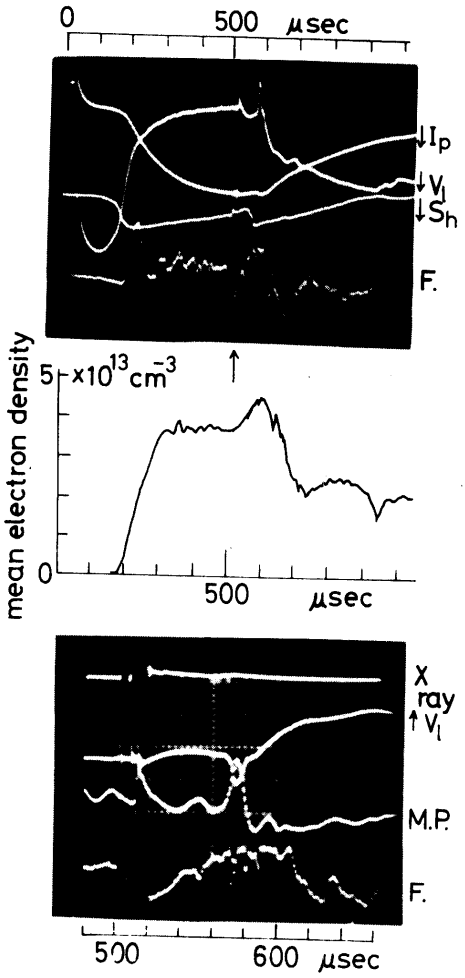
0
500 μsec
↓Ip
↓Vl
↓Sh
F.
mean electron density
5
×10^13 cm^-3
0
500 μsec
X ray
↑Vl
M.P.
F.
500
600 μsec

Fig. 9